Supporting information

Uniform $Pd_{0.33}Ir_{0.67}$ nanoparticles supported on nitrogen-doped carbon with remarkable activity toward alkaline hydrogen oxidation reaction

Yuanyuan Cong,[abc1] Ian T. McCrum,[cd1] Xueqiang Gao,[be1] Yang Lv,[ac] Shu Miao,[f] Zhigang Shao,[b] Baolian Yi,[b] Hongmei Yu,*[b] Michael J. Janik*[cd] and Yujiang Song*[ac]

[a] State Key Laboratory of Fine Chemicals, School of Chemical Engineering, Dalian University of Technology, 2 Linggong Road, Dalian 116024, China.

[b] Fuel Cell System and Engineering Laboratory, Dalian Institute of Chemical Physics, Chinese Academy of Sciences, Dalian 116023, China.

[c] Penn State and DUT Joint Center for Energy Research, Dalian University of Technology, 2 Linggong Road, Dalian 116024, China.

[d] Department of Chemical Engineering, The Pennsylvania State University, University Park, PA 16802, United States.

[e] University of Chinese Academy of Sciences, 19A Yuquan Road, Beijing 100039, China.

[f] Dalian Institute of Chemical Physics, Chinese Academy of Sciences, Dalian 116023, China.

* Corresponding authors: E-mail addresses: hmyu@dicp.ac.cn; mjanik@psu.edu; yjsong@dlut.edu.cn.

[1] These authors contributed equally to this work.

Table of contents

A. Supplementary methods

SI | Extraction of kinetic current density (j_k), mass specific exchange current density ($j_{0,m}$) and area specific exchange current density ($j_{0,s}$)

j_k of alkaline HOR was extracted by reversible Koutecky-Levich equation[1] as follows.

$$\frac{1}{j} = \frac{1}{j_k} + \frac{1}{j_d} \tag{1}$$

Where j is the measured current density, j_k is kinetic current density, j_d is diffusion current density defined as

$$\eta_d = -\frac{RT}{2F} ln\left(1 - \frac{j_d}{j_l}\right) \tag{2}$$

Where η_d is the diffusion overpotential, j_l is the hydrogen mass transport limited current density and can be described by Levich equation[2], F is Faraday's constant, R is the universal gas constant, and T is the temperature.

$j_{0,m}$ was obtained by fitting the kinetic current normalized by metal mass on RDE with respect to the overpotential (η) using the Bulter-Volmer equation as follows,

$$j_k = j_{0,m}\left(e^{\frac{\alpha F}{RT}\eta} - e^{\frac{(\alpha - 1)F}{RT}\eta}\right) \tag{3}$$

where α represents the electron transfer coefficient.

$j_{0,s}$ can be obtained as follows.

$$j_{0,s}(\text{mA cm}^{-2}) = j_{0,m}(\text{A } g^{-1})/(ECSA\ (\text{m}^2\ g^{-1}) \times 10) \tag{4}$$

B. Supplementary figures

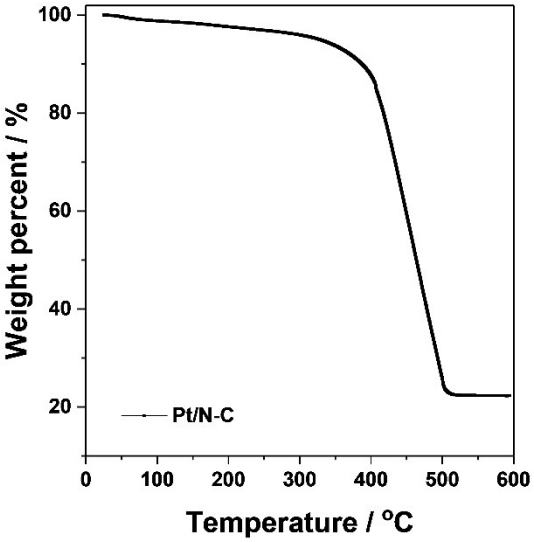

Figure S1. TGA curves of Pt/N-C recorded in dry air with a heating rate of 10 ^{o}C min^{-1}. The residual weight corresponds to the metal loading, which is slightly higher than that of theoretical value in that metal is possibly oxidized during the TGA test.

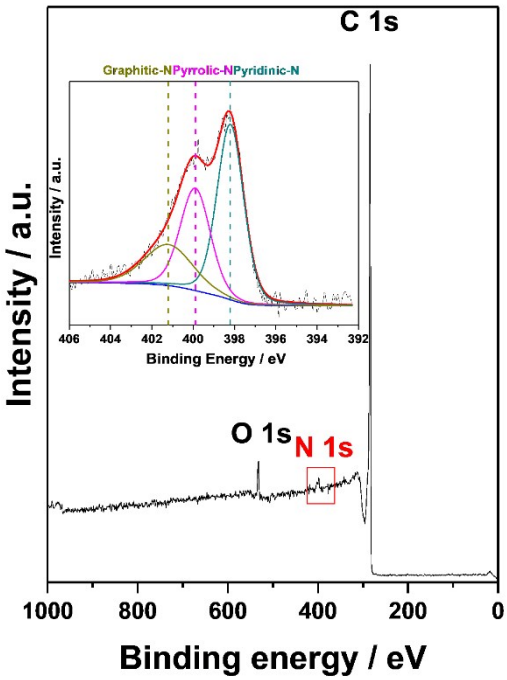

Figure S2. XPS spectrum of N-C (Inset: high-resolution N 1s XPS spectrum).

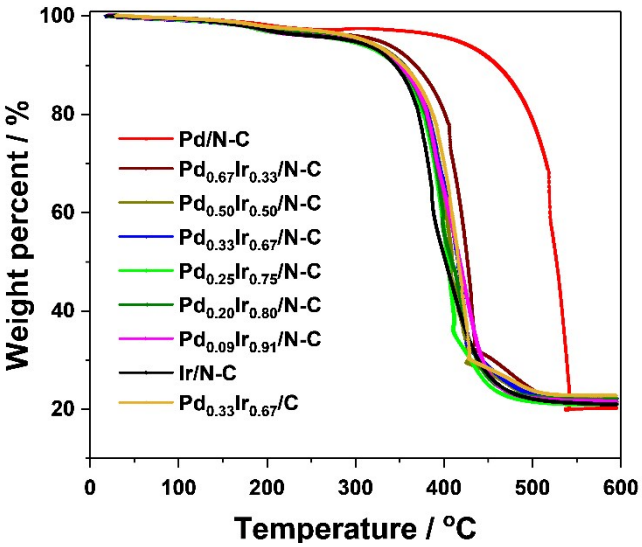

Figure S3. TGA curves of $Pd_{1-x}Ir_x$/N-C (x= 0.33, 0.50, 0.67, 0.75, 0.80, 0.91), Pd/N-C and Ir/N-C recorded in dry air with a heating rate of 10 ^{o}C min^{-1}. The residual weight corresponds to the metal loading, which is slightly higher than that of theoretical value in that metal is possibly oxidized during the TGA test.

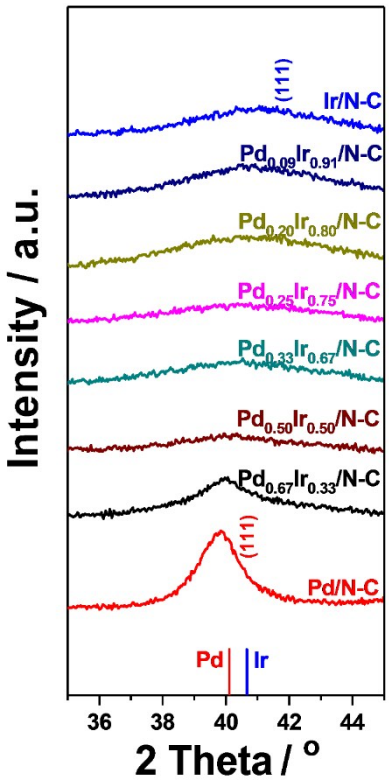

Figure S4. Magnified (111) peak in XRD patterns of $Pd_{1-x}Ir_x$/N-C (x= 0.33, 0.50, 0.67, 0.75, 0.80, 0.91), Pd/N-C and Ir/N-C.

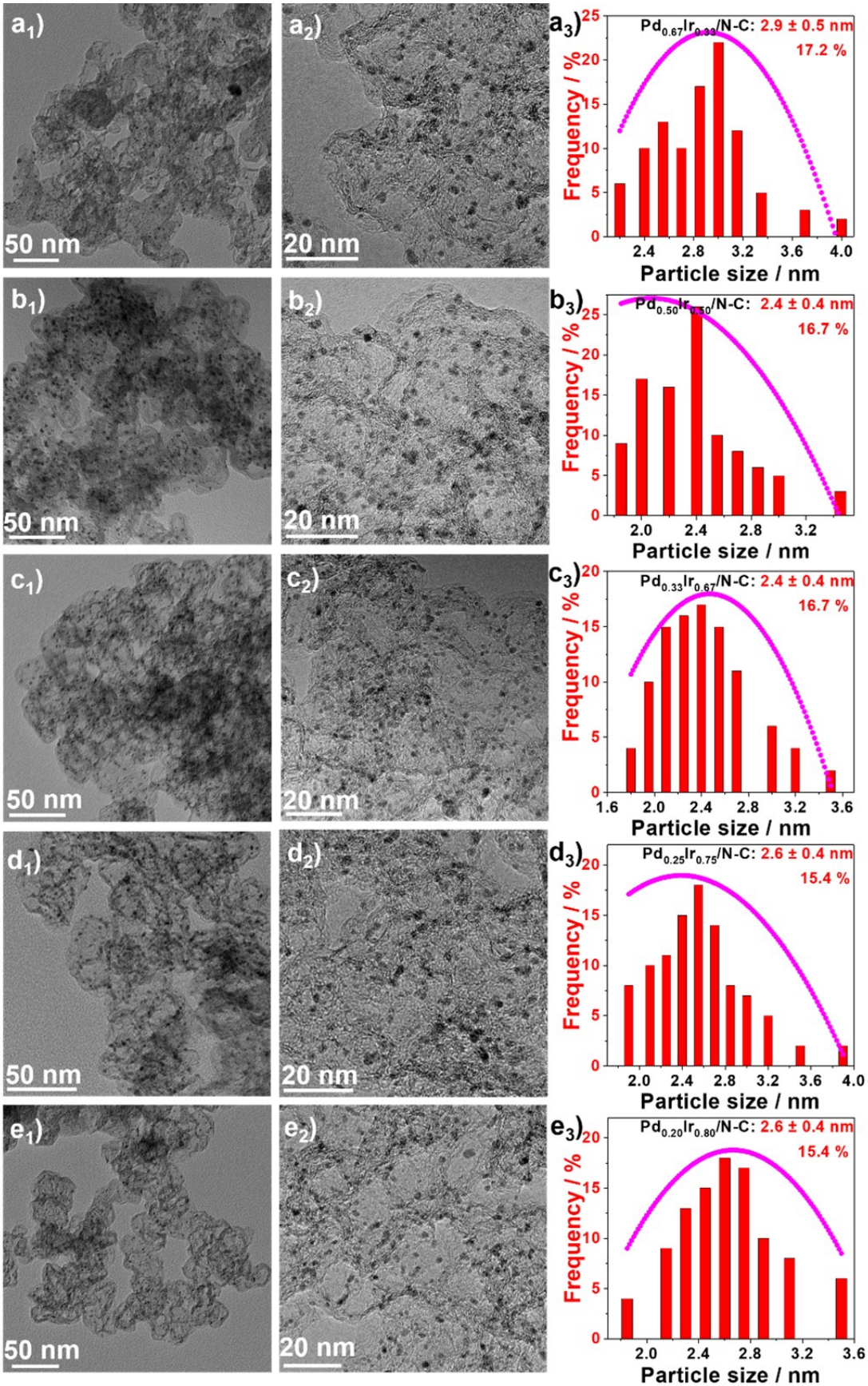
a1)
50 nm
a2)
20 nm
a3)
Pd0.67Ir0.33/N-C: 2.9 ± 0.5 nm
17.2 %
Frequency / %
Particle size / nm
b1)
50 nm
b2)
20 nm
b3)
Pd0.50Ir0.50/N-C: 2.4 ± 0.4 nm
16.7 %
Frequency / %
Particle size / nm
c1)
50 nm
c2)
20 nm
c3)
Pd0.33Ir0.67/N-C: 2.4 ± 0.4 nm
16.7 %
Frequency / %
Particle size / nm
d1)
50 nm
d2)
20 nm
d3)
Pd0.25Ir0.75/N-C: 2.6 ± 0.4 nm
15.4 %
Frequency / %
Particle size / nm
e1)
50 nm
e2)
20 nm
e3)
Pd0.20Ir0.80/N-C: 2.6 ± 0.4 nm
15.4 %
Frequency / %
Particle size / nm

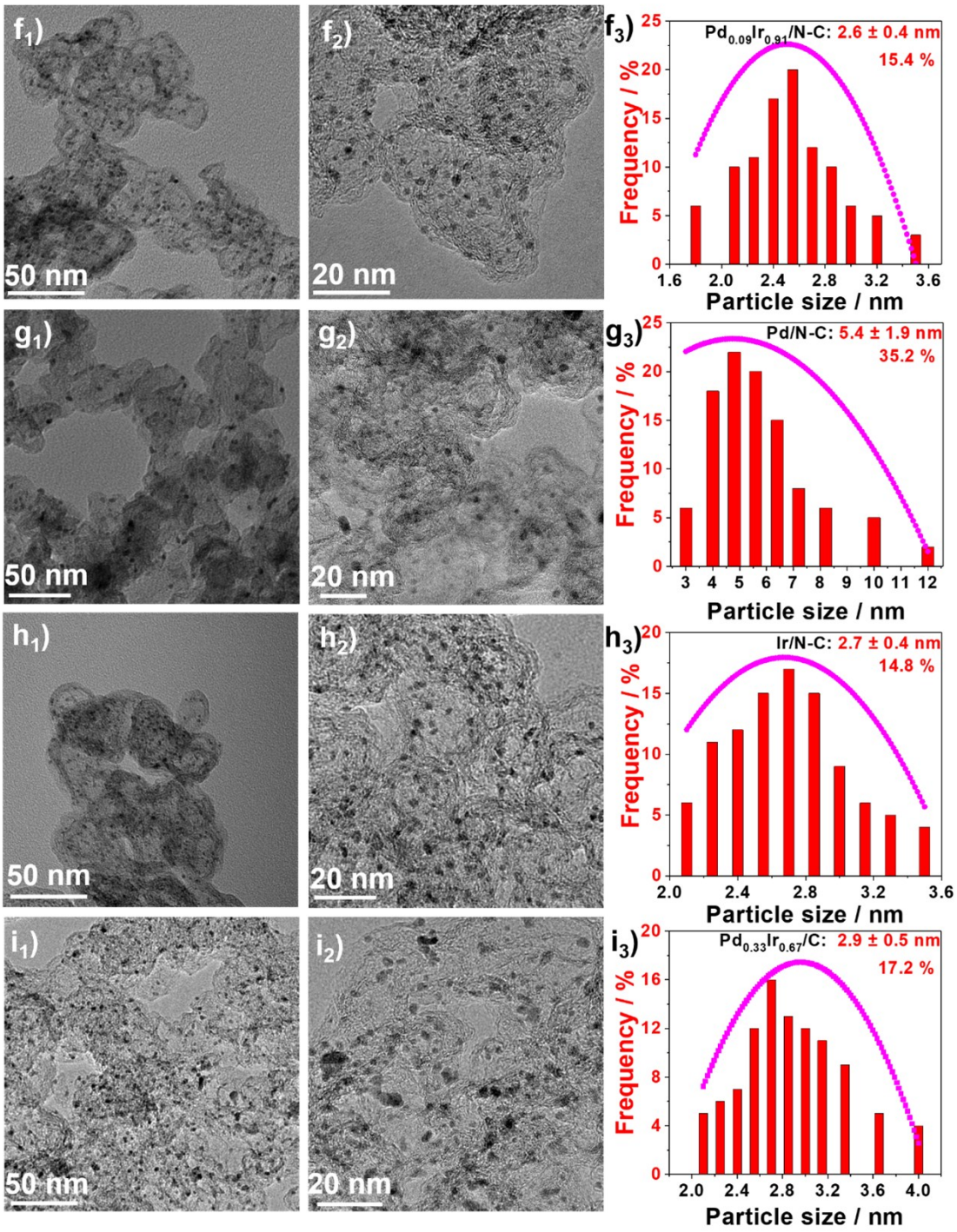

Figure S5. TEM images and corresponding size distribution histograms of $Pd_{0.67}Ir_{0.33}$/N-C (a_1-a_3), $Pd_{0.50}Ir_{0.50}$/N-C (b_1-b_3), $Pd_{0.33}Ir_{0.67}$/N-C (c_1-c_3), $Pd_{0.25}Ir_{0.75}$/N-C (d_1-d_3), $Pd_{0.20}Ir_{0.80}$/N-C (e_1-e_3), $Pd_{0.09}Ir_{0.91}$/N-C (f_1-f_3), Pd/N-C (g_1-g_3), Ir/N-C (h_1-h_3) and $Pd_{0.33}Ir_{0.67}$/C (i_1-i_3).

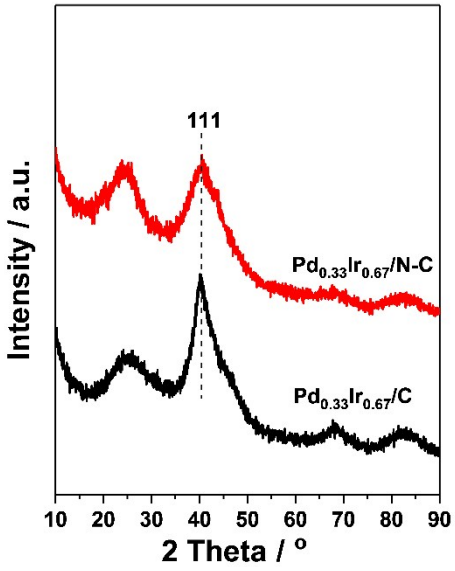

Figure S6. XRD patterns of $Pd_{0.33}Ir_{0.67}$/N-C and $Pd_{0.33}Ir_{0.67}$/C.

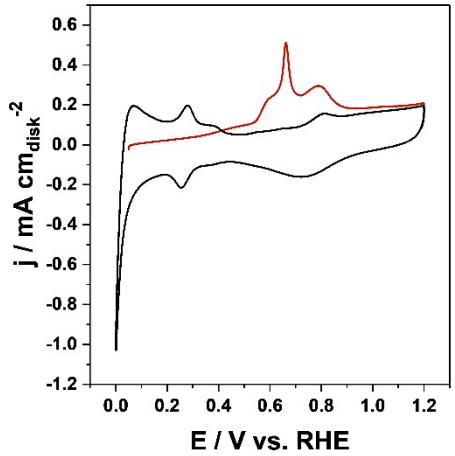

Figure S7. CO stripping voltammetry curves of commercial Pt/C recorded in 0.1 M KOH aqueous solution. Red and black lines are CO stripping and background curves, respectively. Sweep rate: 20 mV s^{-1}, Temperature: 25 °C, Metal loading: 10 μg cm_{disk}^{-2}.

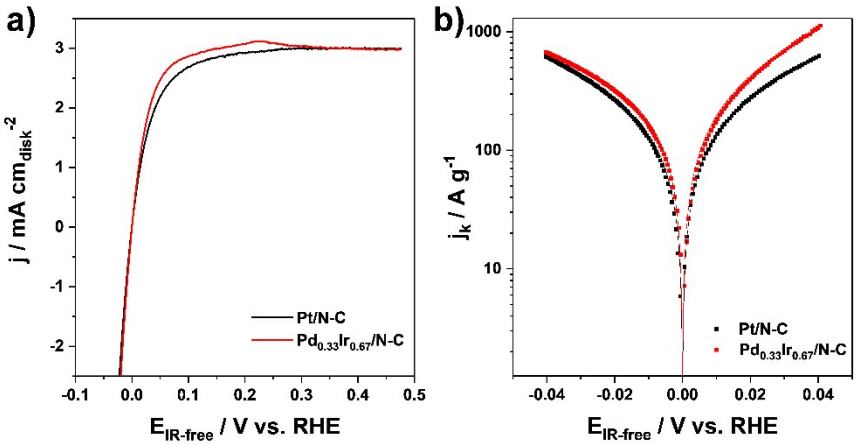

Figure S8. (a) HOR/HER polarization curves of $Pd_{0.33}Ir_{0.67}$/N-C and Pt/N-C recorded in 0.1 M KOH aqueous solution saturated with H_2. Rotation rate: 1600 rpm, Positive sweep rate: 10 mV s^{-1}, Temperature: 25 °C, Metal loading: 10 μg cm_{disk}^{-2}. (b) HOR/HER Tafel plots of $Pd_{0.33}Ir_{0.67}$/N-C and Pt/N-C derived from (a) with kinetic current density fitted into Butler-Volmer equation at $\alpha_a + \alpha_c = 1$ (solid lines).

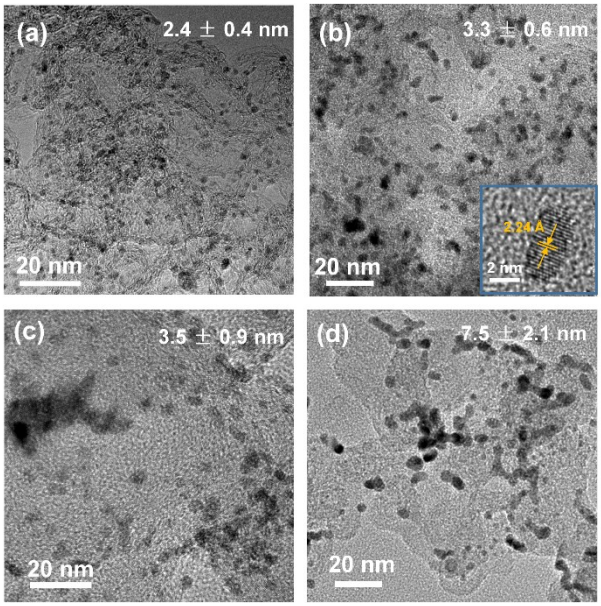

Figure S9. TEM images of $Pd_{0.33}Ir_{0.67}$/C before (a) and after (b) ADT; TEM images of Pt/C before (c) and after (d) ADT. (Inset: HRTEM image of a typical $Pd_{0.33}Ir_{0.67}$ nanoparticle after ADT.

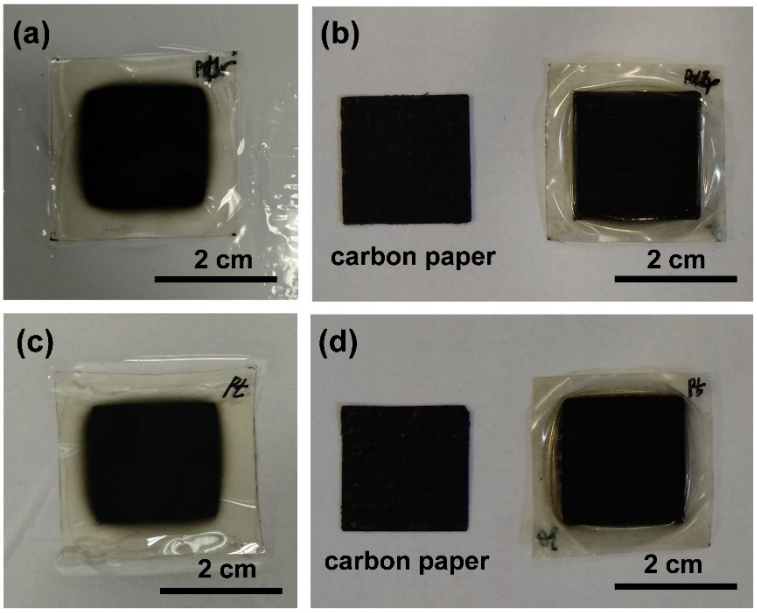

Figure S10. Photographs of $Pd_{0.33}Ir_{0.67}$/N-C before (a) and after (b) single cell tests; photographs of Pt/C before (c) and after (d) single cell tests.

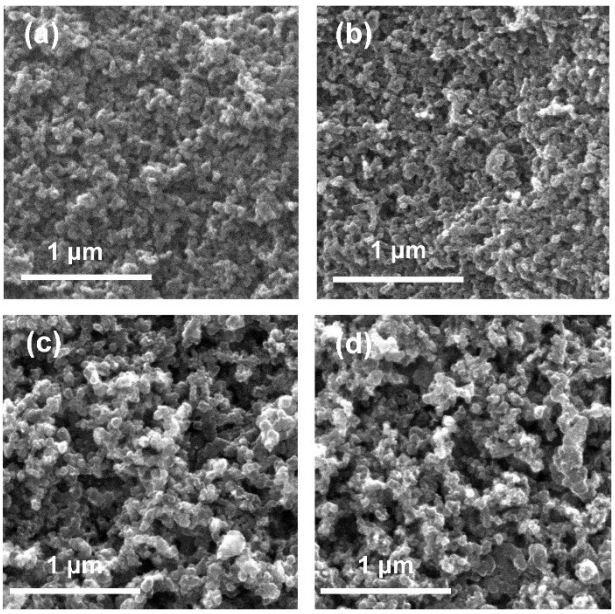

Figure S11. SEM images of anodic $Pd_{0.33}Ir_{0.67}$/N-C catalyst layer before (a) and after (b) single cell tests; SEM images of anodic Pt/C catalyst layer before (c) and after (d) single cell tests.

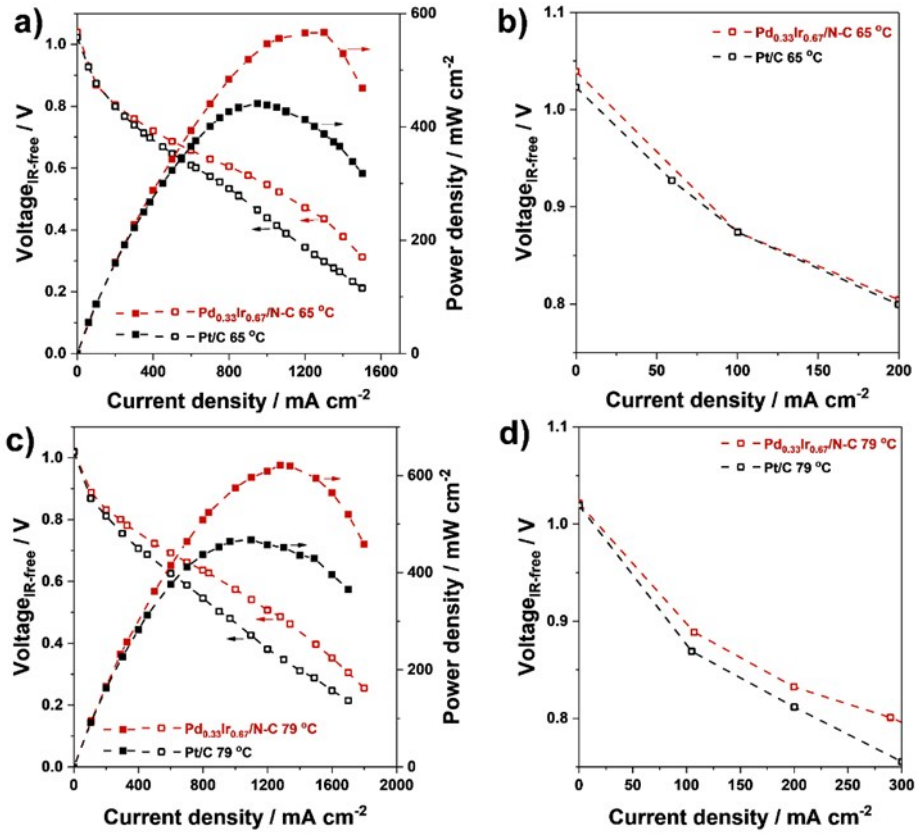

Figure S12. (a) Single cell performance of $Pd_{0.33}Ir_{0.67}$/N-C and commercial Pt/C as anode electrocatalysts at 65 °C after IR-correction and corresponding magnified kinetic region (b); (c) Single cell performance of $Pd_{0.33}Ir_{0.67}$/N-C and commercial Pt/C as anode electrocatalysts at 79 °C after IR-correction and corresponding magnified kinetic region (d).

C. Supplementary tables

Table S1. Pd/Ir ratio and metal loading of $Pd_{1-x}Ir_x$/N-C (x= 0.33, 0.50, 0.67, 0.75, 0.80, 0.91), Pd/N-C, Ir/N-C, $Pd_{0.33}Ir_{0.67}$/C and Pt/N-C

Electrocatalysts	Pd/Ir ratio determined by ICP	Metal loading determined by ICP	Metal loading determined by TGA
Pd/N-C		19.8 %	20.2 %
$Pd_{0.67}Ir_{0.33}$/N-C	0.65/0.35	19.7 %	21.4 %
$Pd_{0.50}Ir_{0.50}$/N-C	0.50/0.50	19.6 %	21.5 %
$Pd_{0.33}Ir_{0.67}$/N-C	0.32/0.68	19.2 %	22.0 %
$Pd_{0.25}Ir_{0.75}$/N-C	0.24/0.76	19.4 %	21.0 %
$Pd_{0.20}Ir_{0.80}$/N-C	0.19/0.81	19.8 %	22.0 %
$Pd_{0.09}Ir_{0.91}$/N-C	0.10/0.90	19.9 %	21.6 %
Ir/N-C		19.7 %	21.0 %
$Pd_{0.33}Ir_{0.67}$/C	0.33/0.67	19.5 %	22.7 %
Pt/N-C		19.8 %	22.2 %

Table S2. The activity data of Pt/C in precious literatures and this study

Electrocatalysts	Area specific activity / H_{upd} ($mA\ cm^{-2}$)	Area specific activity / CO stripping ($mA\ cm^{-2}$)	Mass specific activity ($A\ g^{-1}$)	Ref.
Pt/C	0.05	--	60	[3]
Pt/C	0.57	--	350	[4]
Pt/C	0.46	0.28	294	[5]
Pt/C	0.48	--	240	[6]
Pt/C	0.67	0.38	342	this study

Table S3. ECSAs of $Pd_{1-x}Ir_x$/N-C (x= 0.33, 0.50, 0.67, 0.75, 0.80, 0.91), Pd/N-C, Ir/N-C and commercial Pt/C

	Pd/N-C	$Pd_{0.67}Ir_{0.33}$/N-C	$Pd_{0.50}Ir_{0.50}$/N-C	$Pd_{0.33}Ir_{0.67}$/N-C	$Pd_{0.25}Ir_{0.75}$/N-C
$ECSA_{co}$ ($m^2\ g^{-1}$)	67 ± 7.3	105 ± 18.6	116 ± 6.6	106 ± 10.5	115 ± 4.8
	$Pd_{0.20}Ir_{0.80}$/N-C	$Pd_{0.09}Ir_{0.91}$/N-C	Ir/N-C	Pt/C	
$ECSA_{co}$ ($m^2\ g^{-1}$)	111 ± 5.2	118 ± 7.6	97 ± 13.3	89 ± 8.5	

Table S4. Summary of Pd 3d and Ir 4f binding energies of Pd/N-C, $Pd_{0.33}Ir_{0.67}$/N-C and Ir/N-C from XPS results (Data in brackets represent the relative content of different Pd or Ir species to total Pd or Ir)

Electrocatalysts	Pd $3d_{5/2}$		Ir $4f_{7/2}$	
	Pd^0	Pd^{2+}	Ir^0	Ir^{4+}
Pd/N-C	335.3[a] (50%)	336.2 (50%)		
$Pd_{0.33}Ir_{0.67}$/N-C	335.9 (46%)	337.6 (54%)	61.0 (71%)	62.2 (29%)
Ir/N-C			61.2 (65%)	62.4 (35%)

[a] binding energy (eV)

Table S5. HEMFCs performance with non-Pt and Pt alkaline HOR electrocatalysts reported in literature and this study

Alkaline HOR electrocatalysts	Anode loading (mg_{PGM} cm^{-2})	Backpressure (Mpa)	Temperature (^oC)	Power density (mW cm^{-2})	Ref.
Pd/C-CeO_2	0.3 (higher)	0.3 (higher)	73	500	[7]
Pd/Ni	0.3	0.4	73	400	[8]
IrRu NWs/C	0.1	0.1	60	485	[9]
3 nm Ru/C	0.5	0	50	250	[10]
Pt/C	0.5	0	50	185	[10]
Pt/C	0.1	0	60	233	[11]
Pt/C	0.4_{cat}		45	120	[12]
Pt/C	0.4	0.05	50	370	[13]
Pt/C	1.25 (higher)	0	60	675	[14]
Pt/C	0.4 (higher)	0.1	60	600	[15]
$Pd_{0.33}Ir_{0.67}$/N-C	0.2	0.1	79	514	this study
Pt/C	0.2	0.1	79	400	this study

D. Supplementary references

1 J. Zheng, Y. Yan and B. Xu, *J. Electrochem. Soc.,* 2015, **162**, F1470-F1481.

2 J. Zheng, Z. Zhuang, B. Xu and Y. Yan, *ACS Catal.,* 2015, **5**, 4449-4455.

3 J. Ohyama, T. Sato, Y. Yamamoto, S. Arai and A. Satsuma, *J. Am. Chem. Soc.,* 2013, **135**, 8016-8021.

4 W. Sheng, H. A. Gasteiger and Y. Shao-Horn, *J. Electrochem. Soc.,* 2010, **157**, B1529-B1536.

5 J. Zheng, W. Sheng, Z. Zhuang, B. Xu and Y.Yan, *Sci. Adv.,* 2016, **2**, e1501602.

6 E. G. Mahoney, W. Sheng, Y. Yan and J. G. Chen, *ChemElectroChem,* 2014, **1**, 2058-2063.

7 H. A. Miller, A. Lavacchi, F. Vizza, M. Marelli, B. F. Di, F. D'Acapito, Y. Paska, M. Page and D. R. Dekel, *Angew. Chem. Int. Ed.*, 2016, **55**, 6004-6007.

8 M. Alesker, M. Page, M. Shviro, Y. Paska, G. Gershinsky, D. R. Dekel and D. Zitoun, *J. Power Sources*, 2016, **304**, 332-339.

9 B. Qin, H. Yu, X. Gao, D. Yao, X. Sun, W. Song, B. Yi and Z. Shao, *J. Mater. Chem. A*, 2018, **6**, 20374-20382.

10 J. Ohyama, T. Sato and A. Satsuma, *J. Power Sources,* 2013, **225**, 311-315.

11 B. Qin, H. Yu, J. Jia, X. Gao, D. Yao, X. Sun, W. Song, B. Yi and Z. Shao, *Nanoscale*, 2018, **10**, 4872-4881.

12 I. Kruusenberg, L. Matisen, Q. Shah, A. M. Kannan and K. Tammeveski, *Int. J. Hydrogen Energy* 2012, **37**, 4406-4412.

13 Y. Zhao, H. Yu, F. Xie, Y. Liu, Z. Shao and B. Yi, *J. Power Sources* 2014, **269**, 1-6.

14 T. J. Omasta, L. Wang, X. Peng, C. A. Lewis, J. R. Varcoe and W. E. Mustain, *J. Power Sources,* 2018, **375**, 205-213.

15 Y. Wang, G. Wang, G. Li, B. Huang, J. Pan, Q. Liu, J. Han, L. Xiao, J. Lu and L. Zhuang, *Energy Environ. Sci.,* 2015, **8**, 177-181.